

## Thermally Activated Reorientation of Di-interstitial Defects in Silicon

Jeongnim Kim,<sup>1</sup> Florian Kirchhoff,<sup>2</sup> Wilfried G. Aulbur,<sup>1</sup> John W. Wilkins,<sup>1</sup> Furrugh S. Khan,<sup>2</sup> and Georg Kresse<sup>3</sup>

<sup>1</sup>Department of Physics, The Ohio State University, Columbus, Ohio 43210

<sup>2</sup>Department of Electrical Engineering, The Ohio State University, Columbus, Ohio 43210

<sup>3</sup>Institut für Theoretische Physik, Technische Universität Wien, Wiedner Hauptstraße 8-10/136, A-1040 Wien, Austria

(Received 1 April 1999)

We propose a di-interstitial model for the  $P6$  center commonly observed in ion-implanted silicon. The di-interstitial structure and transition paths between different defect orientations can explain the thermally activated transition of the  $P6$  center from low-temperature  $C_{1h}$  to room-temperature  $D_{2d}$  symmetry. The activation energy for the defect reorientation determined by *ab initio* calculations is 0.5 eV, in agreement with the experiment. Our di-interstitial model establishes a link between point defects and  $\{311\}$  defects, supporting the growth model by interstitial nucleations.

PACS numbers: 61.72.Cc, 61.72.Ji, 71.55.-i

Transient enhanced diffusion (TED) in boron-implanted silicon is the limiting factor in controlling dopant profiles for submicron Si-based devices. Interstitial defects in bulk Si generated during implantation have been identified as the sources for boron TED [1–3]. A class of macroscopical interstitial defects, namely  $\{311\}$  defects, was suggested to emit interstitials that can contribute to the enhancement of boron diffusion under typical implantation conditions [1,2]. Decreasing the ion implantation energy can suppress the formation of macroscopic  $\{311\}$  defects, thus reducing boron TED. However, boron TED exists even at very low implantation energy (below 10 keV) in samples with no visible  $\{311\}$  defects [3]. This implies that microscopic interstitial defects, e.g., interstitial clusters, contribute to boron TED.

The activation energy of boron TED, a measure of the energy required to dissociate interstitials from the interstitial complexes, is lower in samples without visible  $\{311\}$  defects. Interstitial clusters can become important sources for boron TED at low temperature at which the extended  $\{311\}$  defects are still stable against dissociation. Several defect states have been associated with interstitial clusters [4–6]. One of them is the  $P6$  center commonly observed by electron paramagnetic resonance (EPR) measurements in low-energy ion-implanted, proton- or neutron-irradiated silicon [4,5]. The  $P6$  center has  $\{100\}$  symmetry, distinct from the typical  $\{110\}$  symmetry of vacancy-related defects. At low temperature (200 K), the symmetry of the  $P6$  center is either  $C_2$  or  $C_{1h}$  with a twofold axis parallel to the  $\langle 100 \rangle$  direction. A thermally activated symmetry transition occurs at room temperature (300 K) and the symmetry of the  $P6$  center becomes  $D_{2d}$  [7]. Motional averaging effects have been suggested to cause the transition [4,5]. Complementary measurements of the  $^{29}\text{Si}$  hyperfine structure and the stress alignment indicate that the  $P6$  center arises from *di-interstitial* defects. The stable di-interstitial is an important “precursor” of interstitial clusters and more extended defects such as  $\{311\}$  defects. Yet, the structure and dynamics of the di-interstitial

have not been fully understood at an atomic scale and no first-principle calculations are available to our knowledge.

In this Letter, we propose a microscopic structure of a *di-interstitial* whose low-temperature symmetry properties and electronic structure are consistent with the  $P6$  center. Furthermore, the structure and transition paths between different defect orientations (Fig. 1) can account for the experimental symmetry transition to  $D_{2d}$  at room temperature [4,5]. The activation energy of the defect reorientation in our model is 0.5 eV in excellent agreement with 0.6 eV, the experimental activation energy extracted from the response of the  $P6$  center to an external uniaxial

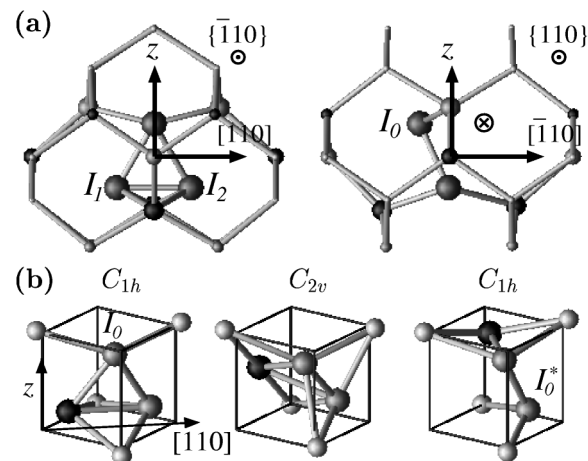


FIG. 1. (a) Atomic structure of a  $C_{1h}$  di-interstitial projected on the  $\{\bar{1}10\}$  and  $\{110\}$  planes and (b) atomic structures of the di-interstitial core during a transition between two  $C_{1h}$  configurations. A regular lattice site located at the origin of the axes is shared by three atoms: (i) the center atom  $I_0$  and (ii) the  $\langle 110 \rangle$  dumbbell atoms  $I_1$ - $I_2$ . The site  $\otimes$  is related to the site  $I_0$  via a mirror reflection across the  $\{\bar{1}10\}$  plane. Three transition paths  $T_x$ ,  $T_y$ , and  $T_z$  with the same energy barrier of 0.5 eV are identified. The  $C_{2v}$  symmetry of the saddle point has a twofold axis parallel to the subscript of the transition  $T_i$ ,  $i = x, y, z$ . For example, the transition  $T_x$  in (b) displaces the center atom  $I_0$  to  $I_0^*$  site and the twofold axis of the saddle point in the middle is parallel to the  $[100]$  direction.

stress [5]. The experimental characterization of the donor level is also consistent with the calculated defect gap states.

The atomic and electronic structure of di-interstitial defects are determined by *ab initio* total energy calculations within the local density approximation (LDA) and generalized gradient approximation (GGA) [8,9]. The local minimum and metastable structures are obtained by structural minimizations using the conjugate gradient method. Starting geometries are stable configurations obtained by molecular dynamics simulations and structural relaxations using tight-binding Hamiltonians [10–12]. In the *ab initio* calculations, the structural minimizations employ two supercell sizes: (i) supercell *A* consisting of 120 atoms and (ii) supercell *B* consisting of 72 atoms. The total energy and structure are well converged with the plane wave energy cutoff of 140 eV and four *k*-points in supercell *A* [13].

Figure 1(a) shows our di-interstitial model of  $C_{1h}$  symmetry, with the twofold axis parallel to the *z* axis [7]. The basic constituents of the model are a center atom  $I_0$  and dumbbell atoms  $I_1$ - $I_2$ . Lee recently proposed a di-interstitial model composed of the same building blocks [5,14]. Our model differs from Lee's model in (i) the orientation of the dumbbell atoms and (ii) the location of the center atom. The dumbbell structure, aligned parallel to the  $[110]$  direction, resembles the  $\langle 110 \rangle$  interstitialcy, the most stable point defect [15]. Our suggestion that the di-interstitial can be formed when an interstitial is captured by the  $\langle 110 \rangle$  interstitialcy is supported by the positive binding energy of the  $C_{1h}$  di-interstitial with respect to isolated interstitials (Table I).

Four equivalent  $C_{1h}$  di-interstitial configurations, distinguished by the location of the center atom, can be constructed with three interstitials sharing one regular lattice site denoted as *o* in Fig. 2(a). The *low-temperature* symmetry containing a twofold symmetry axis parallel to  $\langle 100 \rangle$  is consistent with the  $C_{1h}$  symmetry of our model [4,5]. Figure 2(b) illustrates the four equivalent sites under  $D_{2d}$  symmetry which the center atom can occupy [7]. Thermal averaging motions among four  $C_{1h}$  configurations with

TABLE I. Di-interstitial (DI) formation energies  $E_f$  and binding energies  $E_b$ . The binding energy is defined as  $E_b = -[E_f - 2E_f(I)]$ , where  $E_f(I)$  is the formation energy of an isolated  $\langle 110 \rangle$  interstitialcy. Supercell *A* consists of 120 bulk atoms, while supercell *B* consists of 72 bulk atoms. The energy barrier  $\Delta$  is the total energy difference between  $C_{1h}$  and  $C_{2v}$  di-interstitials for the same supercell.

		Supercell A		Supercell B	
		LDA	GGA	LDA	GGA
$C_{1h}$ DI	$E_f$	4.93	6.01	4.92	6.03
	$E_b$	1.78	1.86	2.02	2.10
$C_{2v}$ DI	$E_f$	5.40	6.51	5.48	6.60
	$E_b$	1.30	1.36	1.46	1.53
	$\Delta$	0.47	0.50	0.55	0.57
$\langle 110 \rangle I$	$E_f(I)$	3.35	3.93	3.47	4.07

a small activation energy barrier can result in the *room-temperature*  $D_{2d}$  symmetry.

Indeed, we can identify transition paths that lead to the thermal averaging motion between four local minima. Three transitions—denoted as  $T_i$ ,  $i = x, y, z$ , according to the twofold symmetry axis of its saddle point—have the same energy barrier of 0.5 eV.

$T_z$  transition.—The transition from the center atomic site  $I_0$  to its mirror image  $\otimes$ , cf. Fig. 1(a), with respect to the  $\{\bar{1}10\}$  plane can occur by a displacement of the atom  $I_0$  along the  $[\bar{1}10]$  direction. The saddle point of the  $T_z$  transition has  $C_{2v}$  symmetry with a symmetry axis along *z*. The orientation of the dumbbell atoms remains the same after the  $T_z$  transition.

$T_x$  transition [Fig. 1(b)].—A displacement of  $I_1$  along the  $[101]$  direction results in a  $I_0$ - $I_1$  dumbbell pair and the atom  $I_2$  becomes the center atom denoted as  $I_0^*$ . The symmetry axis of the saddle point [ $C_{2v}$  in Fig. 1(b)] is parallel to the  $[100]$  direction. The  $T_y$  transition is similar to the  $T_x$  transition,  $I_2$  moving along the  $[011]$  direction. As the result of the  $T_x$  and  $T_y$  transitions, the orientation of the dumbbell atoms changes from the  $[110]$  direction to the  $[\bar{1}10]$  direction.

The *room-temperature*  $D_{2d}$  symmetry can be explained by the thermal averaging motion of three interstitials  $I_0$ ,  $I_1$ , and  $I_2$  alternatively occupying the four center atomic sites [Fig. 2(b)]. Note that the  $T_i$  transitions leading to the thermal motional averaging of the  $D_{2d}$  symmetry involve a displacement of only one of three interstitials along a  $C_{2v}$  saddle point at each transition. The schematics of the potential surface along the high symmetry path is presented in Fig. 3. No other local minima are found along the path  $C_{1h}$ - $C_{2v}$ - $C_{1h}$  for di-interstitial reorientations. The experimental  $D_{2d}$  symmetry is very plausible within our model, since the low transition energy barrier of  $\Delta = 0.5$  eV permits frequent  $T_x$ ,  $T_y$ , and  $T_z$  transitions

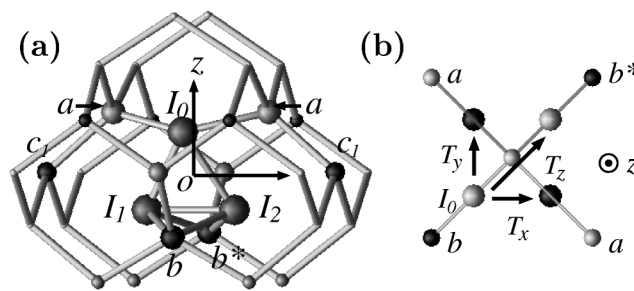


FIG. 2. (a) Atomic structure of a  $C_{1h}$  interstitial and (b) schematics representing the four equivalent sites of the center atom  $I_0$  under  $D_{2d}$  symmetry operations. The regular site indicated by *o* is shared by three interstitials  $I_0$ ,  $I_1$ , and  $I_2$ . The atomic indices are assigned based on the distance from the origin and the symmetry to aid visualization. The experimental  $D_{2d}$  symmetry of the di-interstitial at room temperature can be explained by the thermal averaging motion of  $I_0$ ,  $I_1$ , and  $I_2$  alternatively occupying four equivalent sites. Note that black atoms lie below the gray atoms along the *z* axis.

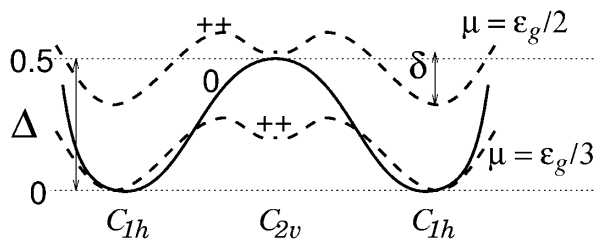


FIG. 3. Schematic potential surfaces along the highly symmetric path of  $C_{1h}$ - $C_{2v}$ - $C_{1h}$  transitions for the neutral state (solid line) and for the positively charged state (dashed lines) at a given chemical potential  $\mu$ . The neutral  $C_{2v}$  di-interstitial is metastable and the energy barrier  $\Delta$  is 0.5 eV. The positively charged  $C_{2v}$  di-interstitial is stable and the energy difference  $\delta$  between  $C_{1h}$  and  $C_{2v}$  di-interstitials is only 0.14 eV.

to motionally average the four  $C_{1h}$  configurations accessible to three interstitials.

We have also determined possible migration processes for di-interstitial diffusion by constant temperature molecular dynamics simulations using a tight-binding potential [12,16]. At 600 K, only di-interstitial reorientations are observed during a 50 psec simulation. At 1200 K, di-interstitial hoppings to the nearest-neighbor sites occur at about 1/5 of the reorientation frequency. Assuming the same entropy factors for the hopping and the reorientation, we obtain an energy barrier  $0.7 \pm 0.1$  eV for the di-interstitial migration [17].

*Structure and energetics of di-interstitial.*—Table I shows the formation energies  $E_f$  and binding energies  $E_b$  of the  $C_{1h}$  di-interstitial, the metastable  $C_{2v}$  di-interstitial, and the  $\langle 110 \rangle$  interstitialcy. Our LDA formation energy of the  $\langle 110 \rangle$  interstitialcy agrees with that obtained by a previous LDA calculation [15]. In general, the bond lengths involved with the defect core atoms  $I_0$ ,  $I_1$ , and  $I_2$  are slightly longer than the bulk bond length of 2.35 Å. Charge density analyses confirm that the defect bonds are indeed weaker than the ideal bulk bonds.

The supercell must be large enough to include third- and fourth-neighbor shell atoms around the defect core. The smaller, 72-atom supercell *B* does not quantitatively describe the energetics and structural properties of the  $C_{1h}$  and  $C_{2v}$  interstitials that were found in the 120-atom supercell *A* and confirmed at the tight-binding level with the 300-atom supercell [13]. Specifically, the transition barrier  $\Delta$  of 0.6 eV in supercell *B* reduces to 0.5 eV in supercell *A* that allows third- and fourth-neighbor shells to relax. That this quantitative difference is a *qualitative* one is evidenced by the bond lengths associated with the defect core differing by as much as 0.3 Å between supercells [18].

We find large discrepancies between LDA and GGA in the formation  $E_f$  and binding energies  $E_b$ , obtained by supercell calculations with a *different number of atoms*. This is attributed to the larger bulk cohesive energy of GGA compared to LDA. On the other hand, the relative stability of the  $C_{1h}$  and  $C_{2v}$  di-interstitials indicated by  $\Delta$  and structural properties are insensitive to the choice

of the exchange-correlation potential  $V_{xc}$ . The formation energy differences between supercells *A* and *B* are of the order of 0.1 eV within LDA. Similar differences are obtained with GGA. The dynamical process for the symmetry transition schematically shown in Fig. 3 is not influenced by  $V_{xc}$ . Typical differences between LDA and GGA results are less than 0.005 Å in bond lengths and less than 0.5° in bond angles for the same supercell size.

*Electronic structure of di-interstitial.*—The experimental analysis of the EPR signal of the positively charged *P6* center indicates that the donor level is strongly localized on the center atom [5]. Figure 4 shows that the defect gap states of the  $C_{1h}$  di-interstitial are strongly localized. The donor level has strong *p* character mostly localized on the atom  $I_0$ , while the acceptor level is mainly localized on the dumbbell atoms  $I_1$ - $I_2$ . The donor level of the  $C_{1h}$  di-interstitial is located at  $E_v + 0.1$  eV and the acceptor level at  $E_v + 0.6$  eV.

For the metastable  $C_{2v}$  di-interstitial, the donor and acceptor levels become almost degenerate and form a deep level at  $E_v + 0.4$  eV. The metastable  $C_{2v}$  di-interstitial

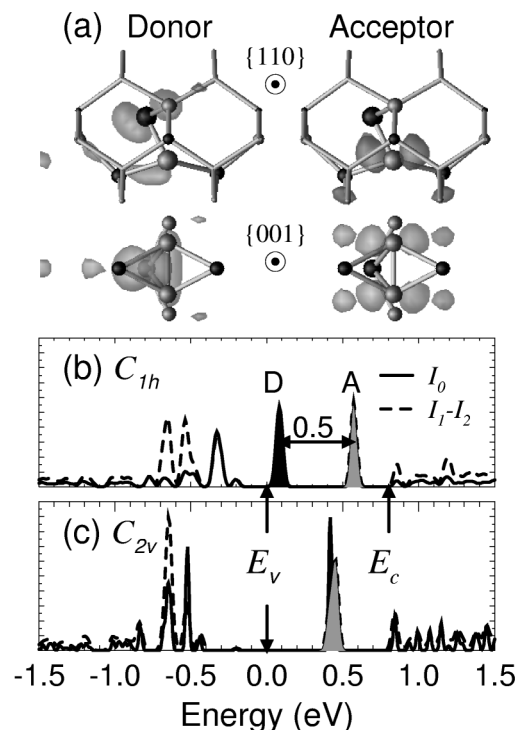


FIG. 4. (a) Isosurfaces of gap state amplitudes of the  $C_{1h}$  di-interstitial, (b) local density of states (LDOS) on the center atom  $I_0$  (solid line) and the dumbbell atoms  $I_1$ - $I_2$  (dashed line) of the  $C_{1h}$  di-interstitial, and (c) those of the  $C_{2v}$  di-interstitial. The reference energy of (b) and (c) is  $E_v$ , the valence band maximum of bulk silicon in the 120-atom supercell *A*. The calculated bulk conduction band minimum,  $E_c$ , is indicated by an arrow and is about 0.8 eV from  $E_v$ . The energy gap of the  $C_{1h}$  di-interstitial is about 0.5 eV, while the donor and acceptor levels of the  $C_{2v}$  di-interstitial are almost degenerate. LDOS of the gap states is highlighted by the black (gray) areas for the donor (acceptor) level.

becomes a stable defect when it is positively charged. The dashed line in Fig. 3 presents a schematic potential surface along the high symmetry path. Self-consistent calculations give a smaller energy difference of 0.14 eV between  $C_{1h}^{++}$  and  $C_{2v}^{++}$  configurations. Our calculations on neutral and doubly charged di-interstitials further support the effective  $D_{2d}$  symmetry of the  $P6$  center even at room temperature.

*Link to extended defects.*—The stable di-interstitial is the link between point defects and extended defects. The dumbbell atoms of the di-interstitial are reminiscent of the  $\langle 110 \rangle$  interstitialcy, suggesting the di-interstitial is formed by an existing  $\langle 110 \rangle$  interstitialcy capturing an interstitial. Previously, we found a stability hierarchy of interstitial defects from molecular dynamics simulations with a tight-binding Hamiltonian [10]: the formation energy decreases in the order of interstitial clusters  $\rightarrow$  interstitial chains  $\rightarrow$   $\{311\}$  defects. First-principle calculations of tri-interstitial defects and interstitial chains further confirm the tight-binding results [19]. This stability hierarchy suggests that the existing interstitial defects can provide nuclei for the formation of  $\{311\}$  defects during a high-temperature annealing process [5,20].

In conclusion, we present first-principle calculations for structural and electronic properties of di-interstitial defects and relate our stable di-interstitial structure to the  $P6$  center. The  $C_{1h}$  di-interstitial model and the transition paths involving the metastable  $C_{2v}$  di-interstitial can account for different symmetries of the  $P6$  center both at low and room temperature. The activation energy of the defect reorientation is 0.5 eV in excellent agreement with experiments. The localization of the donor level also agrees with the experimental characterization.

We wish to thank Dr. Y. H. Lee for useful discussions. This work is supported by the NSF and DOE-BES and computational aids are provided by OSC, NCSA, and NPACI. F. K. acknowledges support by the NRL component of the DoD CHSSI program. The calculations have been performed using the *ab initio* total energy and molecular dynamics program VASP (Vienna *ab initio* simulation program) developed at the Institut für Theoretische Physik of the Technische Universität Wien.

- 
- [1] D.J. Eaglesham, P.A. Stolk, H.-J. Gossmann, and J.M. Poate, Appl. Phys. Lett. **65**, 2305 (1994).
  - [2] P.A. Stolk, H.-J. Gossmann, D.J. Eaglesham, and J.M. Poate, Appl. Phys. Lett. **66**, 568 (1995).
  - [3] L.H. Zhang, K.S. Jones, P.H. Chi, and D.S. Simons, Appl. Phys. Lett. **67**, 2025 (1995).

- [4] Y.H. Lee, N.N. Gerasimenko, and J.W. Corbett, Phys. Rev. B **14**, 4506 (1976).
- [5] Y.H. Lee, Appl. Phys. Lett. **73**, 1119 (1998).
- [6] J.L. Benton *et al.*, J. Appl. Phys. **82**, 120 (1997).
- [7] The twofold axis of the  $C_{1h}$  and  $D_{2d}$  symmetry is chosen to be parallel to  $z = [001]$ . The  $D_{2d}$  group contains two additional twofold axes ( $x$  and  $y$ ) and  $\{110\}$  and  $\{\bar{1}10\}$  reflection planes.
- [8] W. Kohn and L.J. Sham, Phys. Rev. **140**, A1133 (1965).
- [9] G. Kresse and J. Furthmüller, Comput. Mater. Sci. **6**, 15 (1996); G. Kresse and J. Furthmüller, Phys. Rev. B **54**, 11 169 (1996), and references therein.
- [10] J. Kim, J.W. Wilkins, F.S. Khan, and A. Canning, Phys. Rev. B **55**, 16 186 (1997).
- [11] I. Kwon, R. Biswas, C.Z. Wang, K.M. Ho, and C.M. Soukoulis, Phys. Rev. B **49**, 7242 (1994).
- [12] T. Lenosky *et al.*, Phys. Rev. B **55**, 1528 (1997).
- [13] We checked the convergence by increasing the number of  $k$  points to 32 and the plane wave energy cutoff to 200 eV for the 72-atom supercell. The formation energy of the  $\langle 110 \rangle$  interstitialcy changes by 60 meV and the relaxed structure is indistinguishable from calculations using four  $k$ -points and 140 eV. The energy difference between the  $C_{1h}$  and  $C_{2v}$  di-interstitials is converged within a few meV. The structural properties and relative energetics are well converged for supercell  $A$  calculations, confirmed by the less than 10 meV difference in the formation energies between 300- and 120-atom supercell calculations using a TB Hamiltonian of Lenosky *et al.* [12].
- [14] We find the di-interstitial model proposed by Lee [5] is unstable. The local minimum structure obtained by the conjugate gradient minimization under  $C_2$  symmetry constraints has a small binding energy of 0.1 eV.
- [15] J. Zhu, T. Diaz de la Rubia, L.Y. Yang, C. Mailhoit, and G.H. Gilmer, Phys. Rev. B **54**, 4741 (1996), and references therein.
- [16] We find that the tight-binding Hamiltonian by Lenosky *et al.* [12] describes the structures and relative energetics of the di-interstitials and the  $\langle 110 \rangle$  interstitialcy quantitatively well compared to *ab initio* calculations.
- [17] We use the rate equation to estimate the migration energy barrier  $\Delta_m$ :  $e^{-(\Delta_m - \Delta)/k_b T} \sim 1/5$  for  $k_b T = 1200$  K. The estimated error 0.1 eV assumes a range of the relative frequency of the hopping to the reorientation  $1/2 - /20$ .
- [18] The dumbbell atoms in supercell  $B$  are pushed toward the atoms  $b$  and  $b^*$  making long bonds ( $\sim 2.6$  Å) with the next-nearest-neighbor shell atoms.
- [19] Within LDA, the binding energy of a stable tri-interstitial configurations is  $E_b = 2.7$  and that of an infinite interstitial chain is  $E_b = 1.45$  eV.
- [20] M.D. Matthews and S.J. Ashby, Philos. Mag. **27**, 1313 (1973).